

Optimal energy storage and collective charging speedup in the central-spin quantum battery

Hui-Yu Yang,¹ Kun Zhang,^{1,2,3} Xiao-Hui Wang,^{1,2,3,*} and Hai-Long Shi^{4,†}

¹*School of Physics, Northwest University, Xi'an 710127, China*

²*Shaanxi Key Laboratory for Theoretical Physics Frontiers, Xi'an 710127, China*

³*Peng Huanwu Center for Fundamental Theory, Xi'an 710127, China*

⁴*QSTAR, INO-CNR, and LENS, Largo Enrico Fermi 2, 50125 Firenze, Italy*

Quantum batteries (QBs) exploit principles of quantum mechanics to accelerate the charging process and aim to achieve optimal energy storage. However, analytical results for investigating these problems remain lacking due to the challenges associated with nonequilibrium dynamics. In this work, we analytically investigate a central-spin QB model in which N_b spin-1/2 battery cells interact with N_c spin-1/2 charger units, using m initially excited charger units as a resource. By employing the invariant subspace method and the shifted Holstein-Primakoff transformation, we identify four scenarios in which optimal energy storage can be achieved: (i) $N_b \ll m \ll N_c$; (ii) $m \ll N_b \ll N_c$; (iii) $m \ll N_c \ll N_b$; and (iv) $N_b \ll m = kN_c$ [$k \in (0, 1)$]. In these cases, optimal storage is ensured by the SU(2) symmetry emerging from the charging dynamics. The first three cases map the central-spin QB to different Tavis-Cummings (TC) QBs, while the fourth corresponds to the non-TC limit. We analytically determine the charging time and demonstrate that in the fully charging cases (i) and (iv), the collective charging exhibits an N_b -fold enhancement in speedup compared to the parallel charging scheme. Additionally, we numerically observe a unified charging behavior when $m = N_c$, showing that asymptotically optimal energy storage is possible when $N_b = m = N_c$. In this case, we find a collective charging enhancement scaling as $N_b^{0.8264}$. The origin of the collective charging advantage in central-spin quantum batteries is also analyzed through the quantum speed limit and a multipartite entanglement witness. Our results highlight the crucial role of dynamically emergent SU(2) symmetry in providing an analytical understanding of non-equilibrium charging dynamics in QBs.

I. INTRODUCTION

Pioneering theoretical work on energy extraction from many-body states has suggested that the generation of multipartite entanglement can enhance the efficiency of work extraction [1]. This finding implies the existence of a new class of energy storage devices, known as quantum batteries [2] (QBs), which exploit unique quantum features to accelerate the charging process and outperform classical batteries. Compared to charging individual battery cells independently, collective charging exhibits a significant quadratic speedup in charging time [3–6], which is believed to arise from multipartite entanglement induced by collective interactions. The phenomenon where charging power scales faster than the number of quantum cells is referred to as collective charging advantage [7], which has been observed in various models, including the central-spin model [8], spin-chain model [9, 10], Sachdev–Ye–Kitaev model [11], and Dicke model [12–14].

On the other hand, energy storage is another crucial metric for evaluating the performance of a quantum battery [15–17]. Practically, a QB that charges rapidly but stores only minimal energy is not desirable. Recent studies have explored the relationship between energy storage and quantum correlations [15, 18, 19]. However, identi-

fying many-body models that satisfy the conditions for achieving optimal energy storage remains challenging. Here optimal energy storage refers to a situation where the battery absorbs all the energy initially stored in the charger or reaches a fully charged state, which will be rigorously defined later. Our recent work has shown that the emergence of SU(2) symmetry in the Tavis-Cummings (TC) model guarantees the realization of optimal energy storage [16]. Could this emergent symmetry also explain the presence of optimal energy storage in other models? Moreover, under conditions of optimal energy storage, can we achieve collective charging speedup simultaneously? We aim to address these questions in an important low-dimensional model.

The central-spin model has provided significant insights into the quantitative understanding of decoherence in nitrogen-vacancy (NV) centers in diamond, as well as the dynamics of entanglement [20–34]. This model can be naturally put into the framework of QBs, referred to as the central-spin QB, where N_b central spins act as battery cells and N_c bath spins serve as charging units. It has been argued that a collective charging advantage is present in this model; however, the analysis is based on applying the Holstein-Primakoff (HP) transformation to both the bath and central spins [8], which is valid only in the short-time regime and does not extend to the time scale including maximal energy storage [18]. On the other hand, the use of the HP approximation simplifies the central-spin model to the TC model, which we refer to as the TC limit. As discussed in Ref. [16], even within

* xhwang@nwu.edu.cn

† hailong.shi@ino.cnr.it

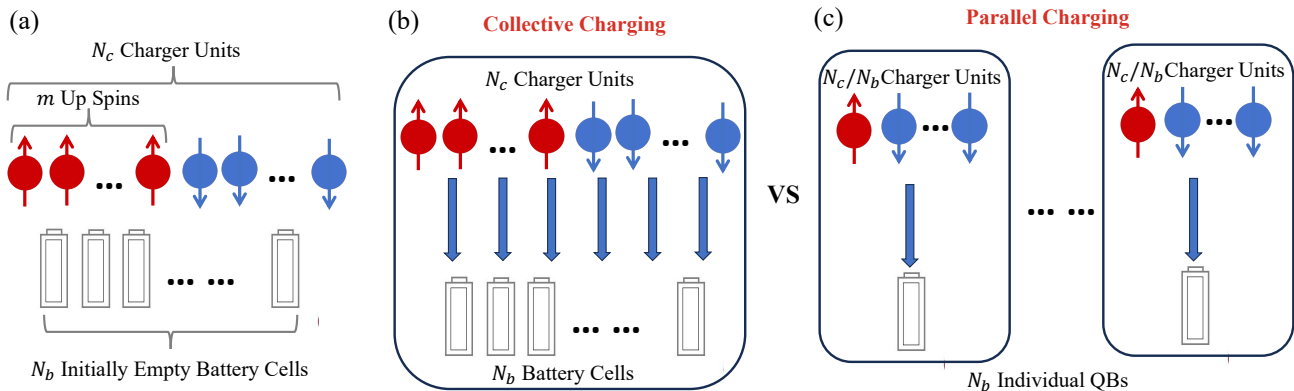


FIG. 1. Schematic diagram of the central-spin QB. (a) Initially, the system consists of N_b battery cells in their ground states, with no excitations, and N_c charger units prepared in a Dicke state containing m excitations. Also shown is a comparison between (b) the collective charging scheme and (c) the parallel charging scheme.

the TC model, optimal energy storage is not guaranteed in all cases. In a specific non-TC limit [35], we identified an optimal energy storage scenario for the case of $N_b=2$ and conjectured, based on numerical evidence, that optimal energy storage persists under this condition for the arbitrary N_b case [35]. The corresponding charging time has also been conjectured and numerically validated. Despite these results, analytical results regarding the conditions for optimal energy storage and the determination of charging time in the central-spin model remain lacking. In particular, can we provide rigorous proof for the conditions and charging time for optimal energy storage in the non-TC limit? Additionally, even for the TC limit, different initial configurations in the central-spin model can be used to realize it. Do these various configurations all guarantee optimal energy storage? Do they yield the same charging time? Addressing these questions will help distinguish the central-spin model from its behavior under the TC limit and deepen our understanding of the nonequilibrium dynamics in the central-spin model.

In this paper we address these questions systematically. In Sec. II we introduce the central-spin model and the invariant subspace approach used for the subsequent analysis. The quantities that characterize optimal energy storage and the collective charging advantage are also given. Section III employs the HP transformation to identify four initial configurations that achieve the TC limits. For the first three cases, we rigorously demonstrate the emergent $SU(2)$ symmetry that ensures optimal energy storage and analytically determine the corresponding charging time. Based on these findings, we prove that the collective charging advantage scales with N_b in the first fully charged TC limit. For the fourth case, numerical calculations indicate the absence of optimal energy storage. In Sec. IV we explore the non-TC limits. We analytically demonstrate a novel scenario for achieving optimal energy storage while maintaining an N_b scaling for the collective charging advantage. Additionally, numerical analysis reveals another non-TC configuration

that attains asymptotic optimal energy storage, with a collective charging advantage scaling as $N_b^{0.8264}$. The origin of the collective charging advantage is discussed in Sec. V using the quantum speed limit and a multipartite entanglement witness. A summary is given in Sec. VI.

II. CENTRAL-SPIN QUANTUM BATTERY

The central-spin QB is described by the Hamiltonian

$$\begin{aligned}
 H &= H_b + H_c + H_I, \\
 H_b &= \omega_b S^z, \\
 H_c &= \omega_c J^z, \\
 H_I &= A(S^+ J^- + S^- J^+),
 \end{aligned} \tag{1}$$

where H_b , H_c , and H_I correspond to the Hamiltonian of the battery, charger, and their homogeneous flip-flop spin interactions in the x - y plane, respectively. Here, $S^\alpha = \sum_{j=1}^{N_b} \sigma_j^\alpha / 2$ and $J^\alpha = \sum_{k=1}^{N_c} \sigma_k^\alpha / 2$ with $\alpha = x, y, z$ are the collective spin operators for the N_b spin-1/2 battery cells and N_c spin-1/2 charger units, respectively. The spin ladder operators are given by $J^\pm = J^x \pm iJ^y$ and $S^\pm = S^x \pm iS^y$.

Initially, the battery is set to the ground state of H_b with N_b spins down, namely, $|0\rangle_b \equiv |\downarrow_1, \downarrow_2, \dots, \downarrow_{N_b}\rangle_b$, while the charger is prepared in a high-energy Dicke state $|m\rangle_c$ with m spins up [see Fig.1(a)]. The charging dynamics is performed by turning on the interactions H_I . To ensure that the energy injected into the battery exclusively comes from the charger, we require $[H_b + H_c, H] = 0$ and thus we only consider the resonant case with $\omega_b = \omega_c \equiv \omega$. Therefore, the free part in the Hamiltonian (1) is a constant and we will ignore it. In terms of the invariant subspace $\mathcal{H}_m = \{|0\rangle_b |m\rangle_c, |1\rangle_b |m-1\rangle_c, \dots, |d\rangle_b |m-d\rangle_c\}$ containing the initial state $|\psi(0)\rangle = |0\rangle_b |m\rangle_c$, the Hamiltonian H defined in Eq. (1) can be represented as a $(d+1) \times (d+1)$ matrix in the invariant subspace \mathcal{H}_m

by using the Dicke basis

$$\mathbf{H} = \begin{pmatrix} 0 & u_1 & & & \\ u_1 & 0 & u_2 & & \\ & \ddots & \ddots & \ddots & \\ & & u_{d-1} & 0 & u_d \\ & & & u_d & 0 \end{pmatrix}, \quad (2)$$

where we have shifted the ground-state energy to cancel the diagonal terms. The off-diagonal terms are given by

$$u_j(N_b, N_c, m) = A\sqrt{j(N_b - j + 1)(N_c - m + j)(m - j + 1)}. \quad (3)$$

The dimension of the effective Hamiltonian (2) is $d+1$ with $d \equiv \min\{N_b, m\}$, which scales linearly with the minimal number of battery cells or the charger units. Then it is easy to diagonalize \mathbf{H} to calculate the dynamics

$$\boldsymbol{\psi}(t) = e^{-i\mathbf{H}t}(1 \ 0 \ \dots \ 0)^T. \quad (4)$$

Thus, the evolution of the total quantum state is expressed as

$$|\psi(t)\rangle = \boldsymbol{\psi}_0(t)|0\rangle_b|m\rangle_c + \dots + \boldsymbol{\psi}_d(t)|d\rangle_b|m-d\rangle_c. \quad (5)$$

The reduced density matrix of the battery state is then obtained as

$$\begin{aligned} \rho_b(t) &\equiv \text{Tr}_c[|\psi(t)\rangle\langle\psi(t)|] \\ &= |\boldsymbol{\psi}_0(t)|^2|0\rangle\langle 0| + \dots + |\boldsymbol{\psi}_d(t)|^2|d\rangle\langle d|. \end{aligned} \quad (6)$$

The energy transferred from the charger to the battery is given by

$$\Delta E(t) = \langle\psi(t)|H_b|\psi(t)\rangle - \langle\psi(0)|H_b|\psi(0)\rangle, \quad (7)$$

where H_b denotes the Hamiltonian of the battery. The charging time, denoted by T , is defined as the time required to achieve the maximum value of $\Delta E(t)$. At the charging time T , the charger has injected as much energy as possible into the battery. However, optimal energy storage occurs only in the following two cases: (i) The battery absorbs all the energy initially stored in the charger or (ii) the battery absorbs some energy from the charger and reaches a fully charged state $|\uparrow \dots \uparrow\rangle$. To quantify the performance of stored energy, we define $\eta(t)$ as

$$\eta(t) \equiv \frac{\Delta E(t)}{\langle\psi_{\text{opt}}|H_b|\psi_{\text{opt}}\rangle - \langle\psi(0)|H_b|\psi(0)\rangle}, \quad (8)$$

where the denominator represents the optimal energy storage, given by $\omega \min\{N_b, m\}$, and $|\psi_{\text{opt}}\rangle = |\min\{N_b, m\}\rangle_b|m - \min\{N_b, m\}\rangle_c$ is the optimal charged state. Therefore, the condition for optimal charging can be expressed as $\eta(T) = 1$. One of our main goals is to analytically determine which types of initial states can achieve optimal energy storage.

Under the restriction of optimal energy storage, our second goal is to demonstrate the collective charging advantage analytically. In the collective charging scheme, shown in Fig.1(b), N_b battery cells collectively interact with N_c charging units, with the charger initially having m spins in the excited state. The collective charging power is defined as

$$P_{\#}(N_b, N_c, m) \equiv \frac{\Delta E(T)}{T(N_b, N_c, m)}, \quad (9)$$

which depends solely on the battery size N_b , the charger size N_c , and the initial number of excited charger spins m . For a fair comparison, the resources used in the parallel charging scheme [see Fig. 1(c)] must be equivalent to those used in the collective charging scheme. In the parallel charging scheme, there are N_b individual single-cell QBs, where each battery cell interacts with N_c/N_b charger units, with m/N_b spins initially excited. To make sense for this setting, we require that $N_c \geq N_b$ and $m \geq N_b$, and we will define the collective charging advantage (12) only for this case. According to Ref. [35], the charging power for a single-cell central-spin QB is given by

$$\begin{aligned} P_{\text{single-cell}} &= \frac{2\omega}{\pi} u_1(1, N_c/N_b, m/N_b) \\ &= \frac{2\omega A}{\pi} \sqrt{\frac{m}{N_b} \left(\frac{N_c}{N_b} - \frac{m}{N_b} + 1 \right)}. \end{aligned} \quad (10)$$

In the parallel charging scheme, the charging time remains the same as in the single-cell QB case, but the total stored energy will be N_b times larger. Therefore, the parallel charging power is given by

$$P_{\parallel} \equiv N_b P_{\text{single-cell}}. \quad (11)$$

The collective charging advantage is thus quantified by

$$\Gamma = \frac{P_{\#}}{P_{\parallel}} = \frac{P_{\#}}{N_b P_{\text{single-cell}}}. \quad (12)$$

If $\Gamma \sim N_b^\alpha$ with $\alpha > 0$, we say the collective charging advantage exists.

III. OPTIMAL ENERGY STORAGE AND COLLECTIVE CHARGING SPEEDUP AT TC LIMITS

In previous work [35] we analytically demonstrated a case of optimal energy storage for $2 = N_b \ll m \ll N_c$ and numerically verified the case of $N_b \ll m \ll N_c$ with arbitrary N_b to achieve optimal energy storage. However, the corresponding charging time was not determined. Actually, under these initial conditions, the central-spin model can be mapped to the TC model, which we refer to as the TC limit. In this section we extend our previous work to find more TC limits and then we use the theory developed in Ref. [16] to determine not only the possibility for

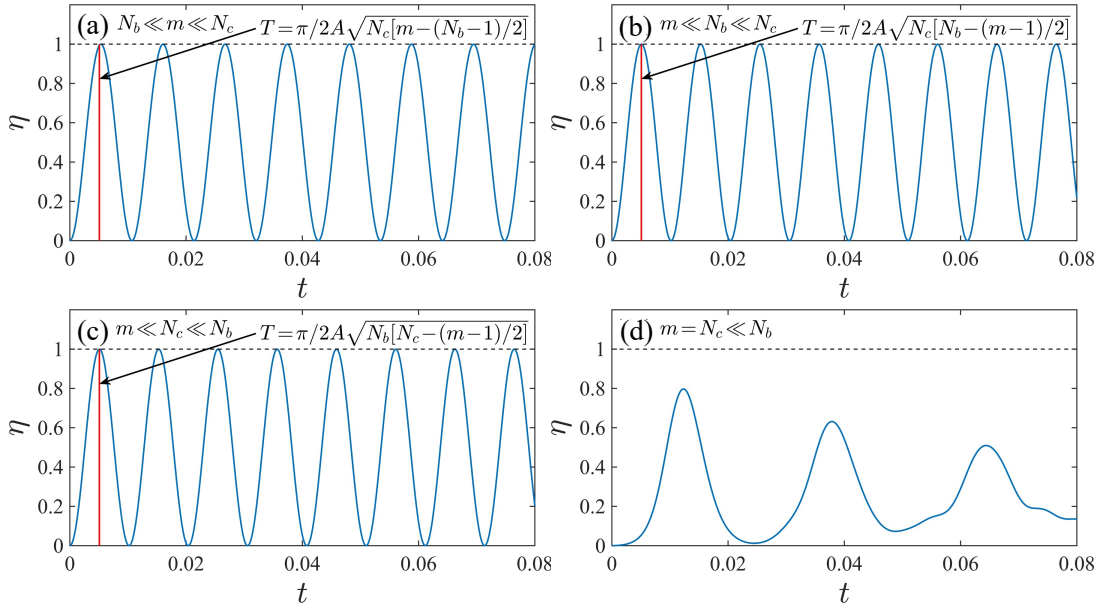


FIG. 2. Charging dynamics for four TC limits: (a) $N_b \ll m \ll N_c$; (b) $m \ll N_b \ll N_c$; (c) $m \ll N_c \ll N_b$; and (d) $m = N_c \ll N_b$. The blue lines are numerically obtained and the red lines are theoretical results. The coupling strength is set to $A=1$.

achieving optimal energy storage but also the collective charging advantage. We emphasize that the emergent $SU(2)$ symmetry in the dynamics plays a crucial role in achieving optimal energy storage and is key to analytically calculating the collective charging advantage.

For the case of $N_b \ll m \ll N_c$, due to the conservation of the total excitation number $[J^z + S^z, H] = 0$, the number of excitations in the charger part cannot exceed the initial value m . Since $\lim_{N_c \rightarrow \infty} m/N_c = 0$, the charger remains close to the vacuum state $|0\rangle_c$ throughout the dynamics at the limit $N_c \rightarrow \infty$. Therefore, we can apply the HP transformation to the charger Hamiltonian as

$$\begin{aligned} J^+ &\rightarrow \sqrt{N_c} a^\dagger \sqrt{1 - \frac{a^\dagger a}{N_c}}, \\ J^z &\rightarrow -\frac{N_c}{2} + a^\dagger a, \end{aligned} \quad (13)$$

where $\sqrt{1 - a^\dagger a/N_c} \simeq 1$ because $\langle \psi(t) | a^\dagger a | \psi(t) \rangle / N_c = \langle \psi(t) | J^z | \psi(t) \rangle / N_c + 1/2 \leq m/N_c \rightarrow 0$. Under this approximation, the original Hamiltonian (1) reduces to

$$H \xrightarrow{N_b \ll m \ll N_c} A \sqrt{N_c} (S^+ a + S^- a^\dagger), \quad (14)$$

where a and a^\dagger are bosonic annihilation and creation operators, respectively. In this correspondence, the number of charger spin excitations m in the initial state $|\psi(0)\rangle = |0\rangle_b |m\rangle_c$ corresponds to the photon number. In Ref. [16] we have shown that for TC battery (14) and initial state $|\psi_{TC}(0)\rangle = |0\rangle_b |n_0\rangle_c$, with $|n_0\rangle$ being a Fock state with n_0 photons, a distinct $SU(2)$ symmetry emerges from the dynamics for the limiting cases $n_0 \gg N_b$

or $N_b \gg n_0$. This results in optimal energy storage given by $\Delta E(T_{TC}) = \omega \min\{N_b, n_0\}$ with the charging time

$$T_{TC} = \frac{\pi}{2A\sqrt{N_c} \sqrt{\max\{N_b, n_0\} - \frac{\min\{N_b, n_0\} - 1}{2}}}. \quad (15)$$

Therefore, we conclude that optimal energy storage in the central-spin QB can be achieved with the initial state $|\psi(0)\rangle = |0\rangle_b |m\rangle_c$, with $N_b \ll m \ll N_c$ [see Fig. 2(a)]. By substituting $n_0 = m$ into Eq. (15), the charging time is given by

$$T(N_b \ll m \ll N_c) = \frac{\pi}{2A\sqrt{N_c} \sqrt{m - \frac{N_b - 1}{2}}}, \quad (16)$$

which is numerically verified in Fig. 2(a). Then by substituting Eqs. (10) and (16) into Eq. (12), the collective charging advantage is obtained as

$$\Gamma(N_b \ll m \ll N_c) = \frac{\sqrt{N_c} \sqrt{m - \frac{N_b - 1}{2}}}{\sqrt{\frac{m}{N_b} \left(\frac{N_c}{N_b} - \frac{m}{N_b} + 1 \right)}} \simeq N_b, \quad (17)$$

which indicates an N_b -fold collective charging speedup compared to the parallel charging scheme.

It is important to emphasize that the TC Hamiltonian (14), which describes the central-spin QB, only requires the number of excited charger spins to be much smaller than the total number of charger spins, i.e., $m \ll N_c$. Moreover, the condition $n_0 \ll N_b$ for optimal energy storage in the TC battery implies another scenario $m \ll N_b \ll N_c$, which also facilitates optimal energy

storage in the central-spin QB [see Fig. 2(b)]. By setting $n_0 = m$ in Eq. (15), we obtain the charging time as

$$T(m \ll N_b \ll N_c) = \frac{\pi}{2A\sqrt{N_c}\sqrt{N_b - \frac{m-1}{2}}}, \quad (18)$$

which is numerically verified in Fig. 2(b). Note that calculating the charging advantage in this case makes no sense because $m/N_b \rightarrow 0$. Therefore, we will only consider the charging advantage for $N_b \leq m$ and $N_b \leq N_c$ in the following discussion.

Unlike the two situations discussed above, we can also employ the HP transformation to map the battery onto a bosonic mode, facilitating the construction of a TC QB from the central-spin QB. Now let us consider the case where $m \ll N_c \ll N_b$. In this regime, the possible maximum excitation for the battery part is m , which is significantly smaller than the battery size N_b . Consequently, the HP transformation can be applied to the battery spins, yielding

$$\begin{aligned} S^+ &\rightarrow \sqrt{N_b} b^\dagger \sqrt{1 - \frac{b^\dagger b}{N_b}}, \\ S^z &\rightarrow -\frac{N_b}{2} + b^\dagger b, \end{aligned} \quad (19)$$

where, by approximating $\sqrt{1 - b^\dagger b/N_b} \simeq 1$, the central-spin QB in Eq. (1) reduces to the TC QB,

$$H \xrightarrow{m \ll N_c \ll N_b} A\sqrt{N_b}(bJ^+ + b^\dagger J^-), \quad (20)$$

where the battery has become a photon field. From the perspective of matrix representation in the invariant subspace [Eq. (2)], the above HP transformation approximates the matrix element u_j as

$$u_j \xrightarrow{m \ll N_b} \frac{A\sqrt{j(N_b - j + 1)(N_c - m + j)(m - j + 1)}}{A\sqrt{N_b}\sqrt{j(N_c - m + j)(m - j + 1)}} \quad (21)$$

with $j = 1, \dots, m$. Considering the additional condition $m \ll N_c$, we can further approximate Eq. (21) as

$$u_j \xrightarrow{m \ll N_c \ll N_b} A\sqrt{N_b}\sqrt{N_c - \frac{m-1}{2}}\sqrt{j(m-j+1)} \quad (22)$$

which implies that the effective Hamiltonian (2) is exactly the generator of the SU(2) algebra

$$H \xrightarrow{m \ll N_c \ll N_b} \sqrt{N_b}\Omega\mathbf{L}^x, \quad (23)$$

where $\Omega \equiv 2A\sqrt{N_c - (m-1)/2}$ is the generalized Rabi frequency and \mathbf{L}^x is the x -direction generator of SU(2) algebra in the spin- m representation. The evolution of energy storage (7) can be represented as

$$\Delta E(t) = \frac{m\omega}{2} + \psi^\dagger(0)\mathbf{L}^z(t)\psi(0)\omega, \quad (24)$$

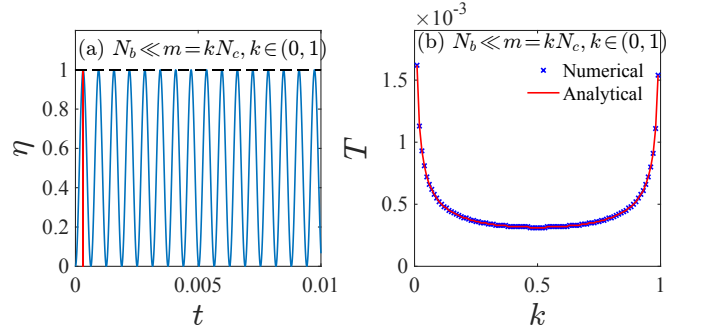


FIG. 3. (a) Charging dynamics in the non-TC limit: $N_b \ll m = kN_c$ with $0 < k < 1$. The blue lines represent numerical results, while the red lines correspond to theoretical predictions. (b) The analytical charging time (36) as a function of k is numerically verified for $N_b \ll m = kN_c$ with $0 < k < 1$. The coupling strength is set to $A = 1$.

where $\mathbf{L}^z(t) = \exp(it\Omega\sqrt{N_b}\mathbf{L}^x)\mathbf{L}^z\exp(-it\Omega\sqrt{N_b}\mathbf{L}^x)$ and $\psi(0) = (1, 0, \dots, 0)^T$. Using the Baker-Campbell-Hausdorff formula, we have

$$\mathbf{L}^z(t) = \sin(\Omega\sqrt{N_b}t)\mathbf{L}^y + \cos(\Omega\sqrt{N_b}t)\mathbf{L}^z, \quad (25)$$

and thus

$$\Delta E(t) = \frac{m\omega}{2}[1 - \cos(\Omega\sqrt{N_b}t)], \quad (26)$$

which implies that optimal energy storage can be achieved at the charging time

$$\begin{aligned} T(m \ll N_c \ll N_b) &= \frac{\pi}{\Omega\sqrt{N_b}} \\ &= \frac{\pi}{2A\sqrt{N_b}\sqrt{N_c - \frac{m-1}{2}}} \end{aligned} \quad (27)$$

[see Fig. 2(c) for numerical verification].

However, we claim that optimal energy storage cannot be achieved in all TC limits, where the emergence of SU(2) symmetry plays a crucial role. As a specific case, we consider the scenario where $m = N_c \ll N_b$. Given the ratio $m/N_b \rightarrow 0$, the maximum possible number of excitations in the battery during the dynamics, i.e., m , is close to zero. Consequently, the effective Hamiltonian remains identical to Eq. (20). Nevertheless, since $m = N_c$ we are unable to apply the same approximation used in deriving Eq. (22). As a result, it is not possible to obtain an SU(2) generator to describe the charging dynamics in this particular TC limit. The absence of SU(2) symmetry in the regime $m = N_c \ll N_b$ therefore prevents the realization of optimal energy storage, as shown in Fig. 2(d).

IV. OPTIMAL ENERGY STORAGE AND COLLECTIVE CHARGING SPEEDUP AT NON-TC LIMITS

Having successfully applied the SU(2) symmetry theory to address the optimal energy storage problem in the

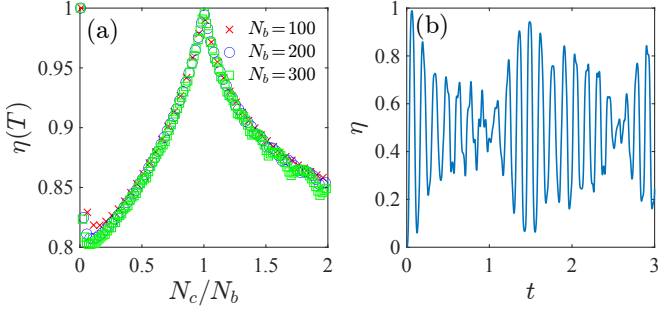


FIG. 4. (a) Maximum energy storage efficiency $\eta(T)$ as a function of N_c/N_b for the case $m = N_b$. (b) Charging dynamics for $m = N_b = N_c = 100$. The coupling strength is set to $A=1$.

TC limits, in this section we use it again to investigate the problem in the non-TC limits. The non-TC limits distinguish the central-spin QB from the TC QB, representing a unique regime specific to the central-spin QB.

The first non-TC limit considered here is $N_b \ll m = kN_c$, with $k \in (0, 1)$. Since $N_b \ll m$, the charger part can be considered essentially unchanged during the dynamics. Therefore, macroscopic excitations are always present in the charger, i.e.,

$$\begin{aligned} & \lim_{N_c \rightarrow \infty} \frac{\langle \psi(t) | \hat{a}^\dagger a | \psi(t) \rangle}{N_c} \\ &= \lim_{N_c \rightarrow \infty} \frac{\langle \psi(t) | J^z | \psi(t) \rangle}{N_c} + \frac{1}{2} = \frac{m}{N_c} = k, \end{aligned} \quad (28)$$

which prevents the direct application of the HP transformation given in Eq. (13). To circumvent this issue, we can first apply the HP transformation (13) and then shift the bosonic operators as

$$\hat{a} = \hat{c} + \sqrt{kN_c}. \quad (29)$$

With this shift, we obtain

$$\begin{aligned} & \lim_{N_c \rightarrow \infty} \frac{\langle \psi(t) | \hat{c}^\dagger c | \psi(t) \rangle}{N_c} \\ &= \lim_{N_c \rightarrow \infty} \frac{\langle \psi(t) | \hat{a}^\dagger a | \psi(t) \rangle}{N_c} - \frac{kN_c}{N_c} = 0. \end{aligned} \quad (30)$$

Substituting Eq. (29) into Eq. (13), we have

$$\begin{aligned} J^+ &= \sqrt{(1-k)N_c} (c^\dagger + \sqrt{kN_c}) \\ &\quad \times \sqrt{1 - \frac{c^\dagger c + \sqrt{kN_c}(c + c^\dagger)}{(1-k)N_c}} \\ &= \sqrt{k(1-k)N_c} + O(\sqrt{N_c}), \end{aligned} \quad (31)$$

where we have used Eq. (30). To leading order in N_c , the central-spin model in Eq. (1) reduces to

$$\begin{aligned} H &\xrightarrow{N_b \ll m = kN_c} A\sqrt{k(1-k)N_c}(S^- + S^+) \\ &= 2A\sqrt{k(1-k)N_c}S^x, \end{aligned} \quad (32)$$

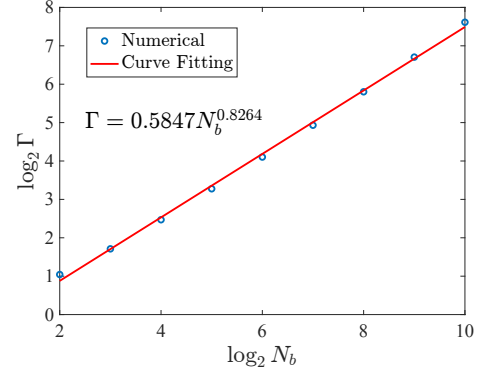


FIG. 5. Scaling of the collective charging advantage Γ as a function of the number of battery cells N_b in the case of $N_b = m = N_c$. The coupling strength is set to $A=1$.

which is exactly the generator of the SU(2) algebra and therefore means that SU(2) symmetry also appears in this non-TC limit. The evolution of energy storage (7) in this case can be expressed as

$$\Delta E(t) = \frac{N_b \omega}{2} + \langle \psi(0) | S^z(t) | \psi(0) \rangle \omega, \quad (33)$$

where $S^z(t) = \exp(itH)S^z \exp(-itH)$. Using the Baker-Campbell-Hausdorff formula, we find

$$\begin{aligned} S^z(t) &= \sin(2A\sqrt{k(1-k)N_c}t)S^y \\ &\quad + \cos(2A\sqrt{k(1-k)N_c}t)S^z. \end{aligned} \quad (34)$$

Thus, the energy evolution is given by

$$\Delta E(t) = \frac{N_b \omega}{2} [1 - \cos(2A\sqrt{k(1-k)N_c}t)], \quad (35)$$

which indicates that optimal energy storage is achieved at the charging time

$$T(N_b \ll m = kN_c) = \frac{\pi}{2AN_c\sqrt{k(1-k)}}, \quad (36)$$

as confirmed numerically in Fig.3(b). Verification of optimal energy storage is shown in Fig. 3(a). By substituting Eq. (36) into Eq. (12), we obtain the collective charging advantage as

$$\Gamma(N_b \ll m = kN_c) = \frac{N_c \sqrt{k(1-k)}}{\sqrt{\frac{m}{N_b} \left(\frac{N_c}{N_b} - \frac{m}{N_b} + 1 \right)}} \simeq N_b. \quad (37)$$

In summary, we show that SU(2) symmetry can also emerge in the non-TC limit, leading to optimal energy storage with a collective charging advantage scaling as N_b .

Note that Eq. (36) does not hold for the case $k=1$, or equivalently $m=N_c$, because the approximation of J^+ is incorrect in this scenario, as the zeroth-order term vanishes. To investigate the region where $m=N_c$, we

perform numerical calculations (see Fig. 4). In Fig. 4(a) we obtain the maximum energy transferred into the battery and plot the energy storage efficiency $\eta(T)$, defined in Eq. (8), at the charging time T for various values of N_b . Surprisingly, $\eta(T)$ exhibits a universal behavior, with all curves collapsing onto a single curve after rescaling. Moreover, we observe that $\eta(T) \rightarrow 1$ for the case $N_c = N_b$, indicating the possibility of achieving optimal energy storage. In Fig. 4(b) we plot the charging dynamics for $N_b = m = N_c$, which shows asymptotic optimal energy storage, meaning that the first maximum of η approaches one. However, due to the absence of dynamically emergent SU(2) symmetry, this case differs significantly from the previous situations and does not exhibit sine like oscillations. In Fig. 5 we plot the collective charging advantage for $N_b = m = N_c$ and find that $\Gamma \propto N_b^{0.8264}$. Although Γ does not scale exactly with N_b in this case, it still demonstrates a collective charging advantage close to an N_b -scaling behavior.

V. ORIGIN OF COLLECTIVE CHARGING ADVANTAGE

We emphasize that there are two distinct origins of the collective charging advantage: the classical origin [7, 12, 36] and the quantum origin [11]. The classical origin arises from the scaling amplification of the norm of the collective charging Hamiltonian, rather than from quantum correlations, such as multipartite entanglement. We argue that the collective charging advantage observed in the central-spin quantum battery is also classical in nature, similar to that of the Dicke battery [13].

The first piece of evidence comes from the quantum speed limit [37, 38]

$$T \geq \frac{\pi \hbar}{2\Delta E}, \quad (38)$$

where T is the charging time, $\hbar=1$ in all calculations, and $\Delta E = \sqrt{\langle \psi(0) | H^2 | \psi(0) \rangle - \langle \psi(0) | H | \psi(0) \rangle^2}$. If the charging time saturates the quantum speed limit, then the charging time T' generated by the dynamics $H' = N_b H$ will be $1/N_b$ times the original charging time T , which is a purely classical effect. Therefore, we introduce the charging rate defined as

$$\gamma \equiv \frac{\tau_{\text{QSL}}}{T} \quad (39)$$

to witness the classical origin of the collective charging advantage, where $\tau_{\text{QSL}} = \pi/2\Delta E$.

A typical parallel charging scheme is governed by Hamiltonian $H_{\parallel} = S^x = \sum_{j=1}^{N_b} \sigma_j^x / 2$. It follows that $T_{\parallel} = \pi$ and $\Delta E_{\parallel} = \sqrt{N_b}/2$. Thus, the typical charging rate for a parallel charging scheme is

$$\gamma_{\parallel} = \frac{1}{\sqrt{N_b}}. \quad (40)$$

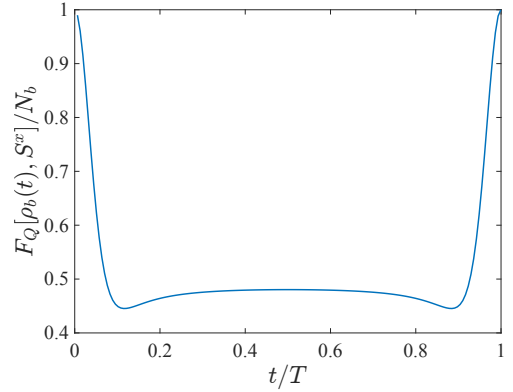


FIG. 6. Evolution of the rescaled QFI for the battery state in the cases of $N_b \ll m \ll N_c$ and $N_b \ll m = kN_c$, in which an N_b -fold enhancement in speedup exists. The number of battery cells is set to $N_b = 50$.

For the collective charging scheme in the central-spin QB, the variance of charging Hamiltonian (1) is given by

$$\begin{aligned} \Delta E &= A \sqrt{\langle 0 | S^- S^+ | 0 \rangle \langle m | J^+ J^- | m \rangle} \\ &= A \sqrt{N_b m (N_c - m + 1)}. \end{aligned} \quad (41)$$

Now we consider the charging rate for two cases with collective charging advantage. The first case corresponds to the TC limit discussed in Sec. III, i.e., $N_b \ll m \ll N_c$. Substituting the charging time (16) into the definition of charging rate (39), we obtain

$$\gamma(N_b \ll m \ll N_c) = \frac{\sqrt{N_c} \sqrt{m - \frac{N_b - 1}{2}}}{\sqrt{N_b m (N_c - m + 1)}} \simeq \frac{1}{\sqrt{N_b}}. \quad (42)$$

The second case corresponds to the non-TC limit $N_b \ll m = kN_c$ discussed in Sec. IV. By substituting the charging time (36) into the charging rate (39), we have

$$\gamma(N_b \ll m = kN_c) = \frac{N_c \sqrt{k(1-k)}}{\sqrt{N_b m (N_c - m + 1)}} \simeq \frac{1}{\sqrt{N_b}}. \quad (43)$$

Since the collective charging rate in the central-spin quantum battery, given by Eqs. (42) and (43), is the same as the parallel charging rate in Eq. (40), we conclude that the collective charging advantage in the central-spin quantum battery is also classical due to the super linear scaling of the bandwidth of the charging Hamiltonian.

The second piece of evidence comes from analyzing the multipartite entanglement structure during the charging dynamics. To witness multipartite entanglement, we adopt the quantum Fisher information (QFI). For a generic N -qubit state $\rho = \sum_{\lambda} q_{\lambda} |\psi_{\lambda}\rangle \langle \psi_{\lambda}|$ (in diagonal form) and an operator \hat{O} , the QFI is given by [39]

$$F_Q[\rho, \hat{O}] = 2 \sum_{\lambda, \lambda'} \frac{(q_{\lambda} - q_{\lambda'})^2}{q_{\lambda} + q_{\lambda'}} |\langle \psi_{\lambda} | \hat{O} | \psi_{\lambda'} \rangle|^2. \quad (44)$$

TABLE I. Optimal energy storage, collective charging advantage, and emergent SU(2) symmetry in the central-spin QB.

Case	Charging Time	Optimal Energy Storage	Emergence SU(2) Symmetry	Collective Charging Advantage
$N_b \ll m \ll N_c$	$\frac{\pi}{2A\sqrt{N_c}\sqrt{m - \frac{N_b-1}{2}}}$	Yes	Yes	N_b
$m \ll N_b \ll N_c$	$\frac{\pi}{2A\sqrt{N_c}\sqrt{N_b - \frac{m-1}{2}}}$	Yes	Yes	NA
$m \ll N_c \ll N_b$	$\frac{\pi}{2A\sqrt{N_b}\sqrt{N_c - \frac{m-1}{2}}}$	Yes	Yes	NA
$m = N_c \ll N_b$	Numerical	No	No	NA
$N_b \ll m = kN_c$ $k \in (0, 1)$	$\frac{\pi}{2AN_c\sqrt{k(1-k)}}$	Yes	Yes	N_b
$m = N_c = N_b$	Numerical	Asymptotically	No	$N_b^{0.8264}$

Violation of the inequality

$$F_Q[\rho_b(t), S^x] \leq sk^2 + r^2, \quad (45)$$

for $\hat{O} = S^x$ indicates that the battery state $\rho_b(t)$ contains at least $(k+1)$ -particle entanglement among the N_b battery cells [40–42], where $s = \lfloor N_b/k \rfloor$ represents the largest integer less than or equal to N_b/k , and $r = N_b - sk$. Therefore, if $F_Q[\rho_b(t), S^x] > N_b$, we can infer the appearance of an entangled battery state. Conversely, if $F_Q[\rho_b(t), S^x] \leq N_b$, we cannot extract useful information about the entanglement structure of $\rho_b(t)$. Actually, QFI is particularly useful for detecting multipartite entangled states close to the Greenberger–Horne–Zeilinger (GHZ)-like states, as the QFI for the GHZ state is N_b^2 , larger than N_b .

Recall the results obtained in the previous sections: We have shown that the appearance of optimal charging is associated with the emergent SU(2) symmetry. In particular, for cases with collective charging advantage, the Hamiltonian in Eq. (2) can be approximated as a generator of SU(2) algebra, i.e.,

$$H \simeq \nu S^x, \quad (46)$$

where $\nu = 2A\sqrt{N_c}\sqrt{m - (N_b - 1)/2}$ for the case of $N_b \ll m \ll N_c$ [43], while $\nu = 2A\sqrt{k(1-k)N_c}$ for the case of $N_b \ll m = kN_c$, as seen in Eq. (32). Based on the effective Hamiltonian in Eq. (46), the evolution of the component of the wave function (4) is obtained as

$$\psi_m(t) = \sqrt{\binom{N_b}{m}} \left[-i \sin\left(\frac{\nu}{2}t\right) \right]^m \left[\cos\left(\frac{\nu}{2}t\right) \right]^{N_b - m}. \quad (47)$$

Therefore, using Eq. (6), the reduced state of the battery is given by

$$\rho_b(t) = \sum_{m=0}^{N_b} q_m(t) |m\rangle\langle m|, \quad (48)$$

with eigenvalues

$$\begin{aligned} q_m(t) &= |\psi_m(t)|^2 \\ &= \binom{N_b}{m} \left[\sin\left(\frac{\nu}{2}t\right) \right]^{2m} \left[\cos\left(\frac{\nu}{2}t\right) \right]^{2N_b - 2m} \end{aligned} \quad (49)$$

Substituting Eq. (48) into the definition of QFI (44), we obtain

$$\begin{aligned} F_Q[\rho_b(t), S^x] &= \sum_{m=0}^{N_b-1} \frac{[q_m(t) - q_{m+1}(t)]^2}{q_m(t) + q_{m+1}(t)} (N_b - m)(m + 1), \end{aligned} \quad (50)$$

where $q_m(t)$ is given in Eq. (49). Figure 6 plots the evolution of QFI for the battery state, given by Eq. (50), which is always less than or equal to N_b . Therefore, a GHZ-like multipartite entanglement structure has not been detected among the battery cells using QFI. With these two pieces of evidence, we conclude that the collective charging advantage observed in the central-spin quantum battery has no genuine quantum origin.

VI. CONCLUSION

In this work we investigated the charging dynamics of a central-spin QB. The problems of optimal energy storage and collective charging advantage were analytically explored within this model. We rigorously demonstrated the realization of optimal energy storage in four different initial state settings: (i) $N_b \ll m \ll N_c$, (ii) $m \ll N_b \ll N_c$, (iii) $m \ll N_c \ll N_b$, and (iv) $N_b \ll m = kN_c$ [$k \in (0, 1)$], where N_b denotes the number of battery cells, N_c represents the number of charger units, and m is the initial number of excited charger units. The first three cases correspond to the TC limits, while the fourth case represents the non-TC limit. Our findings reveal that, across all these cases, the emergence of SU(2) symmetry from the charging dynamics is crucial for achieving optimal energy storage. This emergent symmetry also provides a theoretical approach to analytically determine the charging time. In the fully charged scenarios corresponding to cases (i) and (iv), a collective charging speedup of N_b -fold is proven in comparison to the parallel charging scheme. Furthermore, in the case of $N_b = m = N_c$ we identified the possibility of asymptotically achieving optimal energy storage, with numerical calculations indicating a collective charging advantage scaling as approximately $\sim N_b^{0.8264}$. The main results are summarized in Table I. By employing the quantum speed limit and multipartite

entanglement witness, we identified the classical origin of the collective charging advantage in the central-spin quantum battery. Nevertheless, the classical collective charging advantage is also valuable for designing high-performance quantum batteries [7, 44]. The theoretical central-spin quantum battery in Eq. (1) can be realized in a strongly interacting dipolar spin ensemble [45], where a high-spin NV center can effectively correspond to battery cells, and an ensemble of spin-1/2 P1 centers represent charging units. The key flip-flop spin interactions H_I in Eq. (1) can be realized through the magnetic dipole-dipole interaction between NV and P1 centers. From a practical viewpoint, the case where $N_b = m = N_c$ is the most experimentally favorable for demonstrating both optimal energy storage and the collective charging advantage.

Our work highlights the significance of emergent SU(2) symmetry in analytically addressing the challenges of op-

timal energy storage and collective charging speedup. It extends previous studies on the TC QB [16] and the central-spin QB [35]. We believe the methods used here can be applied to other QB models to uncover further the mechanisms underlying optimal energy storage and collective charging speedup.

ACKNOWLEDGMENTS

HLS thanks Xu Zhou for providing valuable experimental comments. This work was supported by the NSFC (Grants No. 12275215, No. 12305028, and No. 12247103), Shaanxi Fundamental Science Research Project for Mathematics and Physics (Grant No. 22JSZ005) and the Youth Innovation Team of Shaanxi Universities. HLS was supported by the European Commission through the H2020 QuantERA ERA-NET Co-fund in Quantum Technologies project “MENTA”.

-
- [1] K. V. Hovhannisyanyan, M. Perarnau-Llobet, M. Huber, and A. Acín, Entanglement generation is not necessary for optimal work extraction, *Phys. Rev. Lett.* **111**, 240401 (2013).
- [2] R. Alicki and M. Fannes, Entanglement boost for extractable work from ensembles of quantum batteries, *Phys. Rev. E* **87**, 042123 (2013).
- [3] J.-Y. Gyhm, D. Šafránek, and D. Rosa, Quantum charging advantage cannot be extensive without global operations, *Phys. Rev. Lett.* **128**, 140501 (2022).
- [4] F. Campaioli, F. A. Pollock, F. C. Binder, L. Céleri, J. Goold, S. Vinjanampathy, and K. Modi, Enhancing the charging power of quantum batteries, *Phys. Rev. Lett.* **118**, 150601 (2017).
- [5] S. Julià-Farré, T. Salamon, A. Riera, M. N. Bera, and M. Lewenstein, Bounds on the capacity and power of quantum batteries, *Phys. Rev. Res.* **2**, 023113 (2020).
- [6] J.-Y. Gyhm and U. R. Fischer, Beneficial and detrimental entanglement for quantum battery charging, *AVS Quantum Science* **6** (2024).
- [7] F. Campaioli, S. Gherardini, J. Q. Quach, M. Polini, and G. M. Andolina, Colloquium: Quantum batteries, *Rev. Mod. Phys.* **96**, 031001 (2024).
- [8] L. Peng, W.-B. He, S. Chesi, H.-Q. Lin, and X.-W. Guan, Lower and upper bounds of quantum battery power in multiple central spin systems, *Phys. Rev. A* **103**, 052220 (2021).
- [9] T. P. Le, J. Levinsen, K. Modi, M. M. Parish, and F. A. Pollock, Spin-chain model of a many-body quantum battery, *Phys. Rev. A* **97**, 022106 (2018).
- [10] Y. Huangfu and J. Jing, High-capacity and high-power collective charging with spin chargers, *Phys. Rev. E* **104**, 024129 (2021).
- [11] D. Rossini, G. M. Andolina, D. Rosa, M. Carrega, and M. Polini, Quantum advantage in the charging process of sachdev-ye-kitaev batteries, *Phys. Rev. Lett.* **125**, 236402 (2020).
- [12] X. Zhang and M. Blaauboer, Enhanced energy transfer in a dicke quantum battery, *Frontiers in Physics* **10**, 1097564 (2023).
- [13] D. Ferraro, M. Campisi, G. M. Andolina, V. Pellegrini, and M. Polini, High-power collective charging of a solid-state quantum battery, *Phys. Rev. Lett.* **120**, 117702 (2018).
- [14] F.-Q. Dou, Y.-Q. Lu, Y.-J. Wang, and J.-A. Sun, Extended dicke quantum battery with interatomic interactions and driving field, *Phys. Rev. B* **105**, 115405 (2022).
- [15] H.-L. Shi, S. Ding, Q.-K. Wan, X.-H. Wang, and W.-L. Yang, Entanglement, coherence, and extractable work in quantum batteries, *Phys. Rev. Lett.* **129**, 130602 (2022).
- [16] H.-Y. Yang, H.-L. Shi, Q.-K. Wan, K. Zhang, X.-H. Wang, and W.-L. Yang, Optimal energy storage in the tavis-cummings quantum battery, *Phys. Rev. A* **109**, 012204 (2024).
- [17] Z.-G. Lu, G. Tian, X.-Y. Lü, and C. Shang, Topological quantum batteries, arXiv preprint arXiv:2405.03675 (2024).
- [18] G. M. Andolina, M. Keck, A. Mari, M. Campisi, V. Giovannetti, and M. Polini, Extractable work, the role of correlations, and asymptotic freedom in quantum batteries, *Phys. Rev. Lett.* **122**, 047702 (2019).
- [19] D. Šafránek, D. Rosa, and F. C. Binder, Work extraction from unknown quantum sources, *Phys. Rev. Lett.* **130**, 210401 (2023).
- [20] J. Schliemann, A. Khaetskii, and D. Loss, Electron spin dynamics in quantum dots and related nanostructures due to hyperfine interaction with nuclei, *Journal of Physics: Condensed Matter* **15**, R1809 (2003).
- [21] H. T. Quan, Z. Song, X. F. Liu, P. Zanardi, and C. P. Sun, Decay of loschmidt echo enhanced by quantum criticality, *Phys. Rev. Lett.* **96**, 140604 (2006).
- [22] R. Hanson, V. Dobrovitski, A. Feiguin, O. Gywat, and D. Awschalom, Coherent dynamics of a single spin interacting with an adjustable spin bath, *Science* **320**, 352 (2008).
- [23] M. Bortz, S. Eggert, C. Schneider, R. Stübner, and J. Stolze, Dynamics and decoherence in the central spin model using exact methods, *Phys. Rev. B* **82**, 161308

- (2010).
- [24] E. Barnes, L. Cywiński, and S. Das Sarma, Nonperturbative master equation solution of central spin dephasing dynamics, *Phys. Rev. Lett.* **109**, 140403 (2012).
- [25] P. Lu, H.-L. Shi, L. Cao, X.-H. Wang, T. Yang, J. Cao, and W.-L. Yang, Coherence of an extended central spin model with a coupled spin bath, *Phys. Rev. B* **101**, 184307 (2020).
- [26] Q.-K. Wan, H.-L. Shi, X. Zhou, X.-H. Wang, and W.-L. Yang, Decoherence dynamics of entangled quantum states in the xxx central spin model, *Quantum Information Processing* **19**, 400 (2020).
- [27] P. W. Claeys, S. De Baerdemacker, O. E. Araby, and J.-S. Caux, Spin polarization through floquet resonances in a driven central spin model, *Phys. Rev. Lett.* **121**, 080401 (2018).
- [28] N. Wu, X.-W. Guan, and J. Links, Separable and entangled states in the high-spin xx central spin model, *Phys. Rev. B* **101**, 155145 (2020).
- [29] W.-B. He, S. Chesi, H.-Q. Lin, and X.-W. Guan, Exact quantum dynamics of xxz central spin problems, *Phys. Rev. B* **99**, 174308 (2019).
- [30] D. Stanek, C. Raas, and G. S. Uhrig, Dynamics and decoherence in the central spin model in the low-field limit, *Phys. Rev. B* **88**, 155305 (2013).
- [31] F. M. Cucchietti, J. P. Paz, and W. H. Zurek, Decoherence from spin environments, *Phys. Rev. A* **72**, 052113 (2005).
- [32] B. Lee, W. M. Witzel, and S. Das Sarma, Universal pulse sequence to minimize spin dephasing in the central spin decoherence problem, *Phys. Rev. Lett.* **100**, 160505 (2008).
- [33] M. Onizhuk, Y.-X. Wang, J. Nagura, A. A. Clerk, and G. Galli, Understanding central spin decoherence due to interacting dissipative spin baths, *Phys. Rev. Lett.* **132**, 250401 (2024).
- [34] D. Rossini, T. Calarco, V. Giovannetti, S. Montangero, and R. Fazio, Decoherence induced by interacting quantum spin baths, *Phys. Rev. A* **75**, 032333 (2007).
- [35] J.-X. Liu, H.-L. Shi, Y.-H. Shi, X.-H. Wang, and W.-L. Yang, Entanglement and work extraction in the central-spin quantum battery, *Phys. Rev. B* **104**, 245418 (2021).
- [36] G. M. Andolina, M. Keck, A. Mari, V. Giovannetti, and M. Polini, Quantum versus classical many-body batteries, *Phys. Rev. B* **99**, 205437 (2019).
- [37] L. Mandelstam, The uncertainty relation between energy and time in nonrelativistic quantum mechanics, *J. Phys.(USSR)* **9**, 249 (1945).
- [38] S. Deffner and S. Campbell, Quantum speed limits: from heisenberg’s uncertainty principle to optimal quantum control, *Journal of Physics A: Mathematical and Theoretical* **50**, 453001 (2017).
- [39] S. L. Braunstein and C. M. Caves, Statistical distance and the geometry of quantum states, *Phys. Rev. Lett.* **72**, 3439 (1994).
- [40] L. Pezzé and A. Smerzi, Entanglement, nonlinear dynamics, and the heisenberg limit, *Phys. Rev. Lett.* **102**, 100401 (2009).
- [41] G. Tóth, Multipartite entanglement and high-precision metrology, *Phys. Rev. A* **85**, 022322 (2012).
- [42] P. Hyllus, W. Laskowski, R. Krischek, C. Schwemmer, W. Wieczorek, H. Weinfurter, L. Pezzé, and A. Smerzi, Fisher information and multiparticle entanglement, *Phys. Rev. A* **85**, 022321 (2012).
- [43] Please refer to Eq. (14) and substitute $g = A\sqrt{N_c}$, $n_0 = m$ into Eq. (17) of Ref. [16].
- [44] D. Ferraro, M. Campisi, G. M. Andolina, V. Pellegrini, and M. Polini, Reply to the comment on” high-power collective charging of a solid-state quantum battery” by haowei xu and ju li, arXiv preprint arXiv:2412.01830 (2024).
- [45] C. Zu, F. Machado, B. Ye, S. Choi, B. Kobrin, T. Mittiga, S. Hsieh, P. Bhattacharyya, M. Markham, D. Twitchen, *et al.*, Emergent hydrodynamics in a strongly interacting dipolar spin ensemble, *Nature* **597**, 45 (2021).